Electronic Supplementary Material (ESI) for Environmental Science: Water Research & Technology.

Impact of Orthophosphate on the Solubility and Properties of Lead Orthophosphate Nanoparticles

Supplemental Information

Casey L. Formal[1], Darren A. Lytle[2]*, Stephen Harmon[2], David G. Wahman[2], Michael K. DeSantis[2], and Min Tang[3]

Table S1. Literature reported log solubility product constant (K_{sp}) summary for chloropyromorphite, $Pb_5(PO_4)_3Cl$, and hydroxypyromorphite, $Pb_5(PO_4)_3OH$*.

Source	**$Pb_5(PO_4)_3Cl$ log $K_{sp,Cl}$**	**$Pb_5(PO_4)_3OH$ log $K_{sp,OH}$**	**Solid Separation**
Flis *et al.* 2011[1]	–86.5	--	Decantation
Schecher and McAvoy, 1998[2]	–84.43	–62.79	
Nriagu, 1972; Nriagu, 1973[3, 4]	–79.6	–62.83	
Sternleib *et al.*, 2010[5]	–86.5	–65	Centrifuged and supernatant passed through 0.45 µm membrane filter
Topolska *et al.*, 2016[6]	–79.6	--	Decantation
Xie and Giammar, 2007[7]	–80.4	--	0.2 µm membrane filter
Zhu *et al.*, 2015[8]	--	–66.77	0.22 µm membrane filter

* Expressed as: $Pb_5(PO_4)_3OH(s) + H^+ \rightleftharpoons 5Pb^{2+} + 3PO_4^{3-} + H_2O$

References

1. Flis, J.; Manecki, M.; Bajda, T., Solubility of pyromorphite Pb5(PO4)3Cl–mimetite Pb5(AsO4)3Cl solid solution series. *Geochimica et Cosmochimica Acta* **2011,** *75*, (7), 1858-1868.

2. Schecher, W.; McAvoy, D., MINEQL+ Version 4.5. *Environmental Research Software, Hallowell, Maine, USA* **1998**.

3. Nriagu, J. O., Lead orthophosphates. I. Solubility and hydrolysis of secondary lead orthophosphate. *Inorganic Chemistry* **1972,** *11*, (10), 2499-2503.

4. Nriagu, J. O., Lead orthophosphates—II. Stability of chloropyromophite at 25 C. *Geochimica et Cosmochimica Acta* **1973,** *37*, (3), 367-377.

5. Sternlieb, M. P.; Pasteris, J. D.; Williams, B. R.; Krol, K. A.; Yoder, C. H., The structure and solubility of carbonated hydroxyl and chloro lead apatites. *Polyhedron* **2010,** *29*, (11), 2364-2372.

6. Topolska, J.; Manecki, M.; Bajda, T.; Borkiewicz, O.; Budzewski, P., Solubility of pyromorphite Pb5(PO4)3Cl at 5–65°C and its experimentally determined thermodynamic parameters. *The Journal of Chemical Thermodynamics* **2016,** *98*, 282-287.

7. Xie, L.; Giammar, D. E., Equilibrium Solubility and Dissolution Rate of the Lead Phosphate Chloropyromorphite. *Environmental Science & Technology* **2007,** *41*, (23), 8050-8055.

8. Zhu, Y.; Zhu, Z.; Zhao, X.; Liang, Y.; Huang, Y., Characterization, dissolution, and solubility of lead hydroxypyromorphite [Pb5 (PO4) 3OH] at 25–45° C. *Journal of Chemistry* **2015,** *2015*.

Table S2. Lead solubility model equilibria and constants at 25 °C and 0 M ionic strength from Schock, Wagner and Oliphant[26] and references therein, unless otherwise noted.

Name	Equilibrium	log Constant
	Potential Controlling Solids	
$K_{sp,OH}$	$Pb_5(PO_4)_3OH_{(s)} + H^+ \rightleftharpoons 5Pb^{2+} + 3PO_4^{3-} + H_2O$	–62.83
$K_{sp,Cl}$	$Pb_5(PO_4)_3Cl\ (s) \rightleftharpoons 5Pb^{2+} + 3PO_4^{3-} + Cl^-$	–79.6[a]
$K_{sp,HC}$	$Pb_3(CO_3)_2(OH)_2\ (s) + 2H^+ \rightleftharpoons 3Pb^{2+} + 2CO_3^{2-} + 2H_2O$	–18.00
$K_{sp,C}$	$PbCO_3\ (s) \rightleftharpoons Pb^{2+} + CO_3^{2-}$	–13.11
	Hydroxide Complexes	
$\beta_{1,OH}$	$Pb^{2+} + H_2O \rightleftharpoons PbOH^+ + H^+$	–7.22
$\beta_{2,OH}$	$Pb^{2+} + 2H_2O \rightleftharpoons Pb(OH)_{2(aq)} + 2H^+$	–16.91
$\beta_{3,OH}$	$Pb^{2+} + 3H_2O \rightleftharpoons Pb(OH)_3^- + 3H^+$	–28.08
$\beta_{4,OH}$	$Pb^{2+} + 4H_2O \rightleftharpoons Pb(OH)_4^{2-} + 4H^+$	–39.72
$\beta_{2,1,OH}$	$2Pb^{2+} + H_2O \rightleftharpoons Pb_2OH^{3+} + H^+$	–6.36
$\beta_{3,4,OH}$	$3Pb^{2+} + 4H_2O \rightleftharpoons Pb_3(OH)_4^{2+} + 4H^+$	–23.86
$\beta_{4,4,OH}$	$4Pb^{2+} + 4H_2O \rightleftharpoons Pb_4(OH)_4^{4+} + 4H^+$	–20.88
$\beta_{6,8,OH}$	$6Pb^{2+} + 8H_2O \rightleftharpoons Pb_6(OH)_8^{4+} + 8H^+$	–43.62
	Chloride Complexes	
$K_{1,Cl}$	$Pb^{2+} + Cl^- \rightleftharpoons PbCl^+$	1.59
$\beta_{2,Cl}$	$Pb^{2+} + 2Cl^- \rightleftharpoons PbCl_{2(aq)}$	1.80
$\beta_{3,Cl}$	$Pb^{2+} + 3Cl^- \rightleftharpoons PbCl_3^-$	1.71
$\beta_{4,Cl}$	$Pb^{2+} + 4Cl^- \rightleftharpoons PbCl_4^{2-}$	1.43
	Carbonate Complexes and Acid–Base	
K_{c1}	$H_2CO_3^* \rightleftharpoons HCO_3^- + H^+$	–6.355[b]
K_{c2}	$HCO_3^- \rightleftharpoons H^+ + CO_3^{2-}$	–10.336[b]
$K_{1,CO3}$	$Pb^{2+} + H^+ + CO_3^{2-} \rightleftharpoons PbHCO_3^+$	12.59
$K_{2,CO3}$	$Pb^{2+} + CO_3^{2-} \rightleftharpoons PbCO_{3(aq)}$	7.10
$K_{3,CO3}$	$Pb^{2+} + 2CO_3^{2-} \rightleftharpoons Pb(CO_3)_2^{2-}$	10.33
	Phosphate Complexes and Acid–Base	
K_{p1}	$H_3PO_4 \rightleftharpoons H+ + H_2PO_4^-$	–2.141[b]
K_{p2}	$H_2PO_4^- \rightleftharpoons H^+ + HPO_4^{2-}$	–7.200[b]
K_{p3}	$HPO_4^{2-} \rightleftharpoons H^+ + PO_4^{3-}$	–12.338[b]
$K_{1,PO4}$	$Pb^{2+} + H^+ + PO_4^{3-} \rightleftharpoons PbHPO_{4(aq)}$	15.41
$K_{2,PO4}$	$Pb^{2+} + 2H^+ + PO_4^{3-} \rightleftharpoons PbH_2PO_4^+$	21.05

[a] Topolska *et al.*, 2016[29]; [b]Powell, *et al.* (2005)[43]

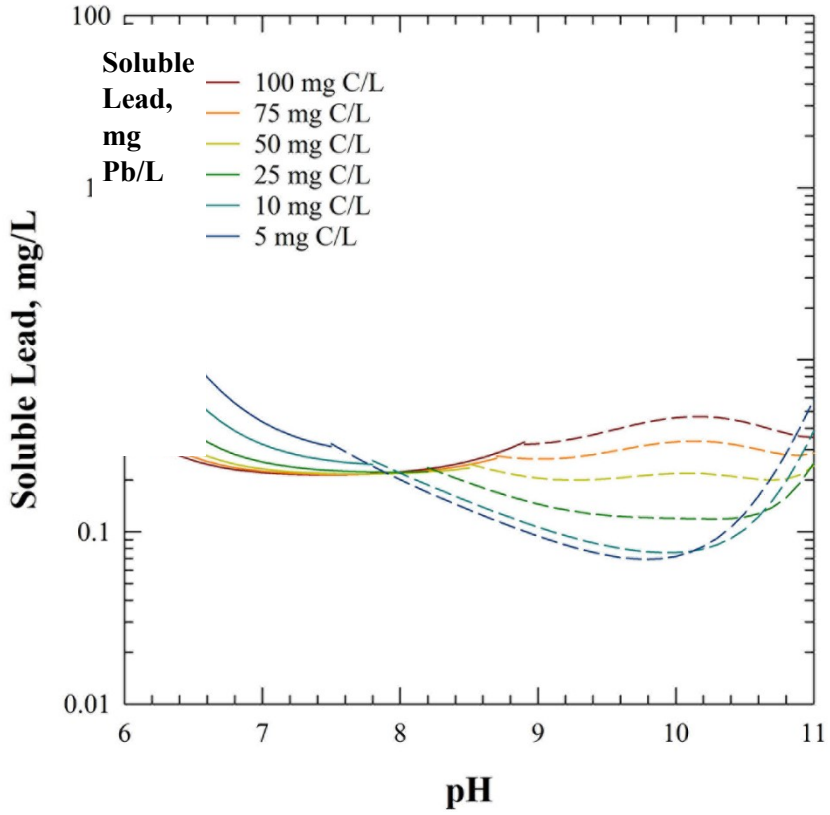

Figure S1. Simulated soluble lead concentrations as a function of pH and dissolved inorganic carbon (mg C/L) concentrations, considering only cerussite (log $K_{sp,C} = -13.11$) or hydrocerussite (log $K_{sp,HC} = -18.00$) as potential controlling solids.[28,29] Solid and dashed lines indicate cerussite or hydrocerussite solid control, respectively.

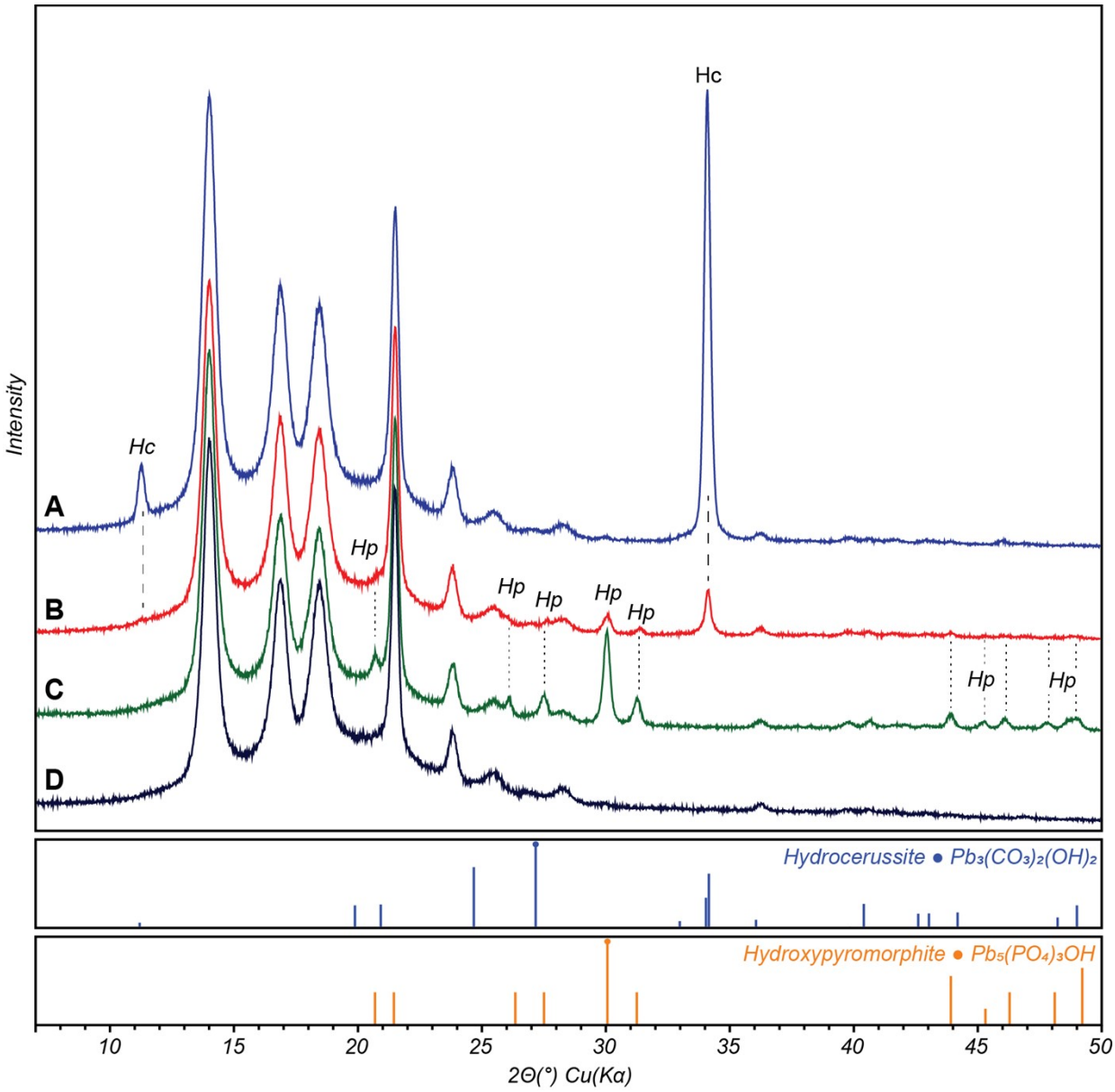

Figure S2. Powder X-ray diffraction (XRD) patterns of selected experiments: (a) 9510, hydrocerussite, the XRD pattern shows only two characteristic hydrocerussite peaks because the platy crystals settled onto the filter in a preferred orientation which accentuated the signal from one crystallographic plane, (b) 95101, mixed hydrocerussite and hydroxypyromorphite, (c) 95102, hydroxypyromorphite, and (d) blank ultrafilter, shows several broad diffraction peaks which are characteristic of the filter material.

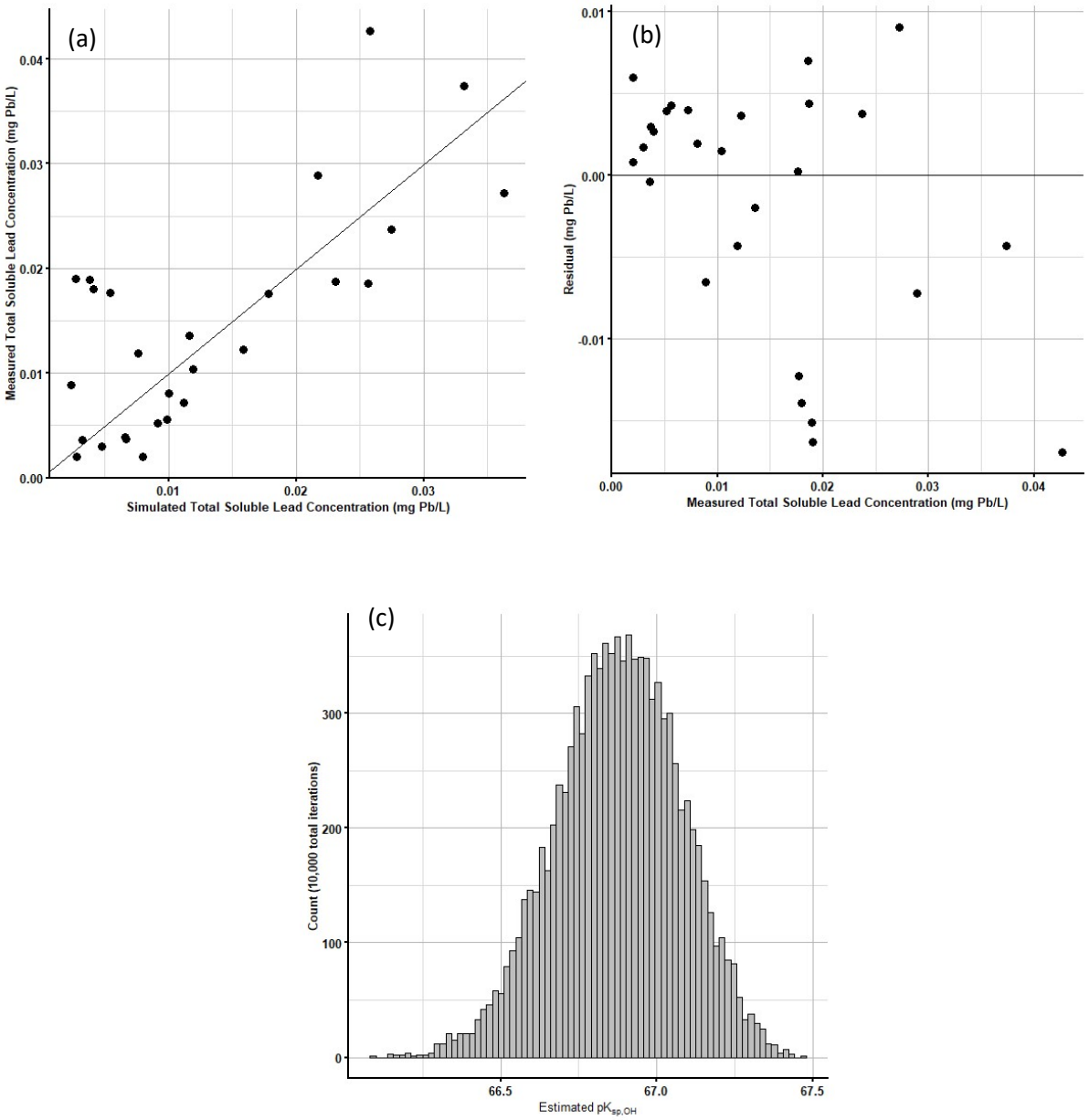

Figure S3. Results from $K_{sp,OH}$ estimation ($10^{-66.87}$): (a) 1:1 correlation plot between experimental data and model simulated total soluble lead concentrations (R^2=0.54), (b) residuals plot of experimental data and model simulated total soluble lead concentrations, and (c) histogram of bootstrap (n = 10,000) results used to determine the 95% confidence interval of the $K_{sp,OH}$ estimate that also illustrates a normal distribution in the estimated $pK_{sp,OH}$ uncertainty.